

MULTIFUNCTION MEASURING METHODOLOGY FOR MONITORING THE CUTTING ZONE WITH DYNAMIC PHENOMENON IN TURNING OF SUPERALLOYS APPLYING THERMOVISION AND HIGH-SPEED SCANNING

Michal Sajgalik, Andrej Czán
Milian Svitana, Peter Ščotka

Summary

Processes in a cutting zone are so complicated and dynamic, that their description is performed by specifically created models. As the models have faults and deviations, it is necessary to improve them so that these deviations become as little as possible or completely abolished and focus on the area of micro-cutting. Examining new ways should be based on the previous research and it is necessary to know the details of the contemporary knowledge. In examining the cutting zone one could widely use nondestructive methods (such as thermovision and high-speed scanning).

Keywords: cutting zone, multifunction measuring, thermo-vision, high-speed scanning

Metodyka pomiarów wielofunkcyjnych w monitorowaniu strefy skrawania z wykorzystaniem zjawisk dynamicznych w procesie toczenia nadstopów z zastosowaniem termowizji i szybkiego skanowania

Streszczenie

Procesy zachodzące w strefie skrawania cechują się dużą dynamiką i złożonością. Stąd są najczęściej definiowane za pomocą specjalnie tworzonych modeli. Jednak same modele z reguły mają usterki i uproszczenia. Z tego względu więc niezbędna jest korekta modeli, dla zmniejszenia skali błędów lub ich całkowitego wyeliminowania. W trakcie poszukiwania nowych metod w opracowaniu modeli należy stosować współczesne możliwości badawcze strefy. Obecnie charakteryzacja strefy skrawania jest prowadzona za pomocą metod nieniszczących, m.in. termowizji i szybkiego skanowania.

Słowa kluczowe: strefa skrawania, pomiary wielofunkcyjne, termowizja, szybkie skanowanie

Address: Andrej Czán, Doc. Eng., Michal Sajgalik, MSc Eng., Milian Svitana, MSc Eng., Peter Ščotka, Eng., Department of Machining and Manufacturing Technology, Faculty of Mechanical Engineering, University of Žilina, Univerzitná 8215/1, 010 26 Žilina, Slovakia, jozef.pilc@fstroj.uniza.sk

1. Processes in cutting zone

1.1 Primary deformation zone

A cutting process is concentrated in an area of contact of a cutting edge of tool with a workpiece. This area is called a cutting zone. As an output from the cutting zone is machined surface and a chip.

The cutting tool effects on workpiece and it causes stress in the material against which the material reacts. As a result the cutting field stabilizes, which has a the strong influence on stress, temperature and deformation.

In the stunted layer front of the cutting wedge, the significant increase of hardness of the material can be observed. This indicates strong hardening. This layer takes the function of the cutting wedge. At high temperature, the plastic deformation field is this layer appears.

In a real process of a chip formation, the whole area is in the plastic state with different intensity of deformation, which is in a stunted layer extremely high. In shear zone hardening is higher than in the middle of the chip element. A boundary of plastic deformation is not really linear, but it is curved toward the workpiece (Fig. 1).

The size of the compression of chip can be determined also in the discontinuous cut. This method is affected by the character of the process and k is different than in the continuous cut [1-7]

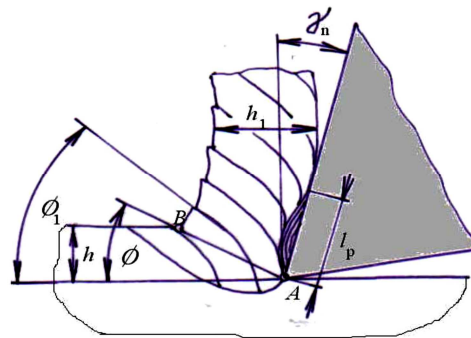


Fig. 1. Scheme of chip formation in continuous cutting: φ – angle of plastic deformation, φ_1 – angle of texture in the chip, h – width of cutting layer, h_1 – width of chip, l – length of contact of rake face with chip

In the front of the cutting wedge there is a deformation zone, which extends to the cutting layer and partly below the machined surface. Boundary of plastic deformation is defined by an angle φ . In the chip, deformed grains skew due to the pressure of the tool at an angle of texture φ_1 (Fig. 1).

Intensity of plastic deformation, in the rough definition, is characterized by the angle of plastic deformation, which indicates positions of the marginal layer above which the material is plastically deformed. It is a significant simplification of the real deformation zone, but for practical computing is adequate. Because there is the plastic deformation, k is always greater than 1.

Extremely shear deformations appearing near the cutting edge. It results in a specific deformation structure in the form of flattened and rounded grains. In fact, the “plastic nose” is participating in cutting of the chip, which has a larger radius r_{mm} than the radius of the real cutting edge r_n . At A , the point of the maximum narrowing of fibers at the cutting edge, the level of deformation achieves critical values, leading to a local rupture (a fiber rupture). A mechanism of deformation and process of breach in a chip formation is continually repeated. This phenomenon is a more pronounced for the existence of a built up edge.

Built up edge arises only at a sufficient plasticity conditioned by the cutting temperature. Area of cutting speed, when the built up edge arises, is in range $20-60 \text{ m} \cdot \text{min}^{-1}$ for the low carbon steel. For roughing, when the surface quality is not significant, the existence of built up edge is less harmful. Built up edge has negative impact on finishing.

The built up edge is formed only when the contact speed of chip on rake face is zero and a force of cutting resistance is directed to the axis of the forming the built up edge.

A course of this process significantly depends on the distribution of temperature in the chip, the tool and the workpiece, respectively, the distribution of heat and friction. Strength of the built up edge is higher than strength of the chip, where the temperature is lower and therefor the flow of material runs over the built up edge. Formation of the built up edge is more probable at the materials where strength increases with temperature [2].

1.2. Secondary deformation zone

Deformation of the chip in the zone of the direct contact between the chip and the rake face is caused by the existence of friction between these two moving bodies. A very important factor, which is in many cases decisive, is the value of the coefficient of friction between the chip and the rake face. In the past it was assumed that the friction between the chip and the rake face can be characterized by a single parameter – the medium angle of friction μ_s .

The course of normal and tangential stresses on the rake face of the orthogonal cutting with-out cooling in the chip formation without the built up edge can be simply defined in Fig. 2.

In the suggested process the stress between last point of contact chip and rake face is zero. Normal stress increases exponentially towards the cutting edge. In the area $(l_n - l) < x < l_n$ stress waveform can be used to determine the coefficient of friction at the rake face by the relation:

$$\frac{\tau}{\sigma} = \mu_s = \text{const.} \quad (1)$$

In the point of a coordinate $x = l_n - l$ normal stress increases so that the contact surface is equal to the real one and tangential stress reaches the material yield stress τ_k . In the area $0 < x < (l_n - l)$ the increase of the normal stress has no effect on the tangential stress, which is constant (Fig. 2).

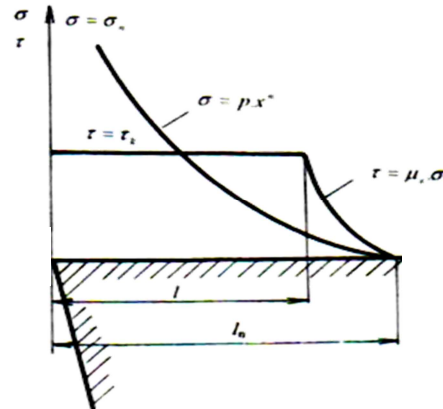


Fig. 2. Hypothetical distribution of stress on the rake face

The plastic flow of the workpiece near the rake face has a significant impact on a chip removal mechanism. In most cases, the plastic flow is associated with other factors, namely heat generation, head distribution and accelerating of material elements. Due to heat distribution from the point of contact, yield of the shear stress strength of the material, leading to higher coefficient of friction and movement of chip elements near the rake face is affected by braking material in contact with the rake face. A boundary layer has a typical shape of the curved fibers (Fig. 3). Accordingly, the texture angle can be exactly determined. It is possible to measure reliably this angle on metallographic sample of chip, because there is not trace of an angle φ , only the φ_r . If the cutting tool has 0° rake angle, the chip indicates the φ angle. If the rake angle is positive, it must be added to the measured value φ_r and the negative angle subtracts it [7].

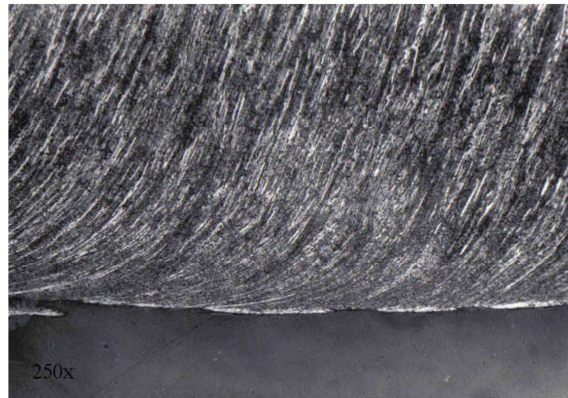


Fig. 3. Metallographic sample of chip:
side adjacent to the rake face (100 Cr 6, $v_c = 100 \text{ m} \cdot \text{min}^{-1}$)

1.3. Thermal field and its distribution

The temperature in the cutting zone is one of the most important parameters affecting the conditions and has an impact on all cutting conditions. The possibility and suitability of the use of cutting speeds, feeds, depth of cut depends on the temperature and the temperature effects on a tool lifetime. It indirectly, but significantly affects productivity and an economic efficiency of production [4].

A mechanical work in machining is transformed into heat, which warms the workpiece and the tool. Because almost the entire quantity of work of plastic deformations and friction in machining is converted into heat, the quantity of heat Q is expressed by:

$$Q = W = F_c \cdot v_c \cdot t \quad (2)$$

where: Q – the total heat, J; F_c – the main component of the cutting force, N; v_c – the cutting speed, $\text{m} \cdot \text{min}^{-1}$; t – the cutting time, min.

In the cutting zone there are three sources of heat:

- from the primary deformation Q_{sh} ,
- from the secondary deformation Q_{tm} (area of chip over the rake face),
- from the friction between the tool surface and the transitional area of workpiece Q_{pln} .

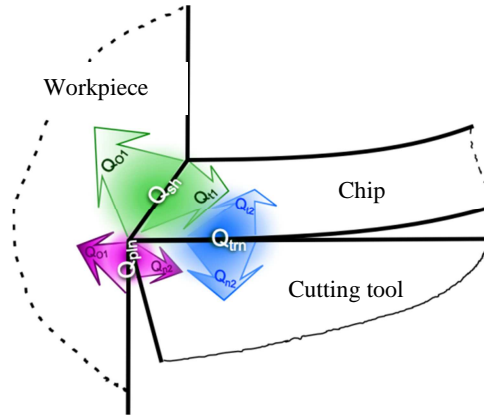


Fig. 4. Sources of heat and its distribution in cutting zone [4]

The heat balance is a form of the energy balance, indicating that the specific location and time period is the amount of dissipation equal to the heat input (Fig. 4). For the conditions in the cutting zone, in machining by the cutting tool with defined geometry the following applies:

$$Q = Q_{sh} + Q_{tm} + Q_{pln} = Q_o + Q_n + Q_t + Q_p \quad (3)$$

where: Q_o – heat in workpiece; Q_n – heat in tool; Q_t – heat in chip; Q_v – exhausted heat.

For the individual components applies:

$$Q_{sh} < Q_{tm} < Q_{pln} \quad (4)$$

The chip receives a substantial part of the heat Q_{sh} and Q_{tm} , because its temperature is highest. A smaller amount of heat (and part of the Q_{tm} and Q_{pln}) is received by the tool. At higher speeds, the heat from the primary deformation is not enough to divert into the workpiece, because the tool cuts the part of the heated material (Fig. 4).

Heat sources from flank are not enough to warm the surface layer of the workpiece. Therefore, the workpiece is the least heated element of a technological system.

Because heating of cutting tool deteriorates its mechanical and cutting properties, it is necessary to eliminate an adverse effect of high temperature by a cooling gas or liquid environment.

For temperature measurement in machining, physical or chemical phenomena can be applied. Due to the difficulty and specific conditions of the

machining processes only certain methods can be used. In the experimental determination and practical measurements the following are used:

- thermoelectric effect (thermocouples),
- change of electrical resistance (thermistors),
- thermal radiation (pyrometers, thermovision),
- change of the structure (thermometers chalks and paints).

1.4. Forces and their action in the cutting zone

The process of chip formation and surface machining is a complicated physical process in which there is an elastic and a plastic deformation in the cutting material layer, and simultaneously the internal friction of chip material and the external friction between contact surfaces of the cutting edge, chip and transitional surfaces of the workpiece. These deformation changes are a consequence of stress in the material. Stress is induced by the external force of tool that enters at a speed into the material of the workpiece.

Overall cutting force of one cutting wedge can be decomposed into three mutually perpendicular components (Fig. 5):

- F_c – *cutting force* – this component is called a tangential or the main cutting force. Knowledge of its values is needed to calculate the power of the main motion, strength of the tool, parts of mechanism of the main cutting motion.
- F_p – *passive force* – called the radial cutting force. Knowledge of its values is needed for calculation of precision machined components. For a free-cutting, this component is zero, since the tool does not move sideways, but only to the axis.
- F_f – *force of feed* – called the axial cutting force. Its size must be known for calculating the adjusting mechanism parts [2].

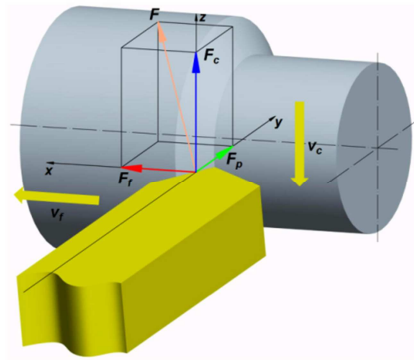


Fig. 5. Components of cutting force in general cutting

Between the cutting force and its components there is the following relation:

$$F = \sqrt{F_c^2 + F_p^2 + F_f^2} \quad (5)$$

The size of components of the cutting force is mainly dependent on cutting parameters (cutting speed, feed and cutting depth), then the geometry of the cutting tool, cutting environment, cutting material, workpiece material, etc. With increasing cutting speed components of cutting force decrease and with increasing, the cutting depth and feed rate they increase.

2. Multifunction measuring system

2.1. Thermovision system

When considering all processes ongoing in the cutting zone, until now it was possible to observe only one kind of processes at a time.

Currently, we can use modern technologies in such a way that it is possible simultaneously in one machining process to measure and monitor all ongoing processes and changes.

Thermovision uses an infrared part of the light spectrum defined as the thermographic spectrum. The infrared radiation, a type of a electromagnetic wave in spectrum covers a wide range (much wider than visible radiation). On the side of shorter wavelengths borders with dark red visible range (wavelength $\lambda = 780$ nm) and on the side of longer wavelengths borders with microwaves spectrum (waves generated by radio sources). Boundaries of the long-waves infrared radiation are not well defined, therefore value of $\lambda = 1$ mm is accepted.

Temperature by touch methods is in some cases very difficult, because contact with controlled elements. Therefore it is necessary to focus on ways to measure of temperature that do not require direct contact with a measured element. Just to capture, display and evaluation the measurements thermal fields, a thermography is used.

Advantages of noncontact measurement of temperature:

- no errors due to imperfect contact,
- there is no danger of destruction of sensors due to the contact with the measured surface,
- measured temperature is available immediately,
- operation of the measuring devices can be far from the measured object,
- from one measuring point, an overview of the temperature distribution from a large area, can be obtained.

- possibility of measuring of very high temperatures, where other methods are insufficient [4].

Almost of all thermovision systems consist of the following parts (Fig. 6):

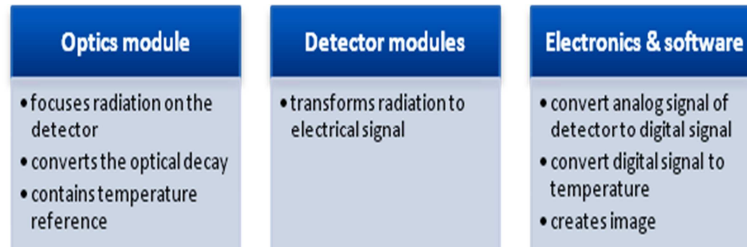


Fig. 6. Scheme of the general thermovision system

In the case of thermography the so-called infrared quantum detectors or simply called the infrared camera or thermovision are used [8].

2.2. High-speed imaging

High-speed imaging in multi-function system runs on two levels: high-speed image capture and high-speed scanning of dynamic components of cutting force.

Principle of image capturing is called “time magnifier” and it is based on capturing with a high frame rate (usually 1000 up to 18 000 frame per second) and consequent slowdown in the current video frame rate (PAL system used in Europe has 25 fps). This way quick action can be monitored and after slowdown to 700 – times deceleration and allow better analysis of these processes [8].

High-speed imaging is performed by a specific CCD or CMOS sensor, which can capture up to 7000 fps in resolution 1024x1024 pixels. Transfer of a signal is indicated in the next Fig. 7.

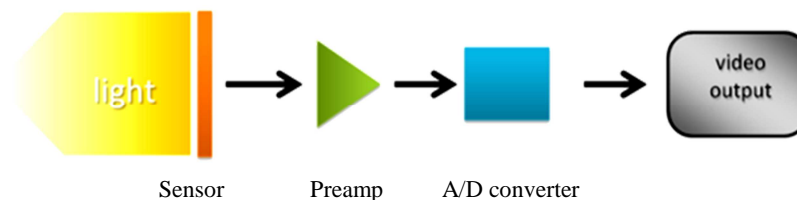


Fig. 7. Scheme of transfer of a signal [9]

The study of micro changes require a carefully prepared side, i.e. a captured workpiece surface (must be polished and etched). To prevent lateral flow of

material and guarantee a constant distance from lens to captured surface, a hard glass plate is usually attached to a side face.

In the case of cameras, according to the theory of photography, the largest chip that is capable to detect lighter signal in short time with less noise is chosen. In the case of examined object, it is necessary to ensure that it is sufficiently lighted, while the frequency of the light source must be higher than the frequency of imaging. In the failure to fulfill this latter condition the “flicker” picture appears on the resulting video [10-12].

3. Conditions of experiments – characteristics of studied materials and of used measurement equipment

In all experiments super-alloys such as nickel and titanium alloys were used (Fig. 8), because they allow monitoring of processes at slow cutting speeds (Fig. 9).

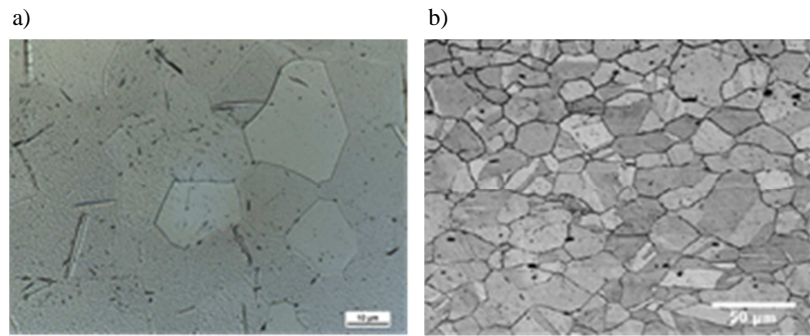


Fig. 8. Microstructure of: a) Ti-GR2 and b) Monel alloy 400

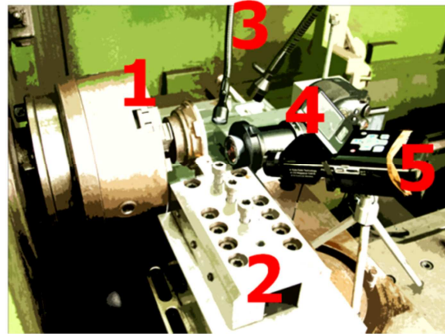


Fig. 9. Multifunction measuring system: 1 – workpiece, 2 – dynamometer with tool, 3 – cold light, 4 – camera with high-speed capturing, 5 – thermovision system

Used measurement system consists of three devices for monitoring process in cutting zone (Fig. 9):

- dynamometer KISTLER 9441 with A/D converter and software interface DASY LAB and computer, which allows to measure up to three components of the cutting force with high-speed scanning,
- camera with high-speed image capturing up to 1000 fps with macro conversion lens RAYNOX MSN-202 with 20x diopters,
- thermovision system MOBIR M8 with “off-axis” lens, which allows to measure the axis up to 1200°C.

This measuring system allows simultaneous measurement of the temperature and the cutting force and monitoring deformations and chip formation in the cutting zone.

Each device has software interface for PC, where we can process and analyze all measured data.

Cutting conditions: Ti-GR2: $v_c = 40 \text{ m}\cdot\text{min}^{-1}$, $a_p = 6 \text{ mm}$, $f = 0.18 \text{ mm}$ and Monel Alloy 400, $v_c = 40 \text{ m}\cdot\text{min}^{-1}$, $a_p = 6 \text{ mm}$, $f = 0.18 \text{ mm}$.

Process of cutting was restricted to free-cutting in turning without cooling on universal lathe. Samples of materials have a thickness 6 mm with diameter 80 mm. Mounting of samples were handled by five screws and shaft (Fig. 10). During the experiments there were measured components of the cutting force, and the temperature area in the cutting zone and there were monitored processes in the cutting zone.

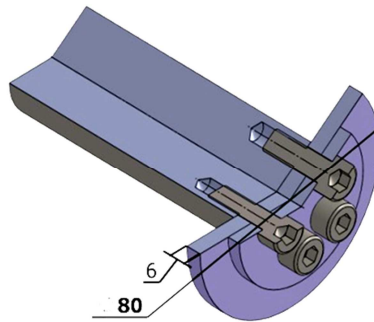


Fig. 10. Schematic view of a part section of sample and preparation for mounting

All experiments were performed in laboratories of Department of Machining and Manufacturing Technologies.

4. Experiments results

4.1. Combined thermal images

Multifunction measuring system allows combining real and thermal images. In Figure 11, we can see a course of turning from the first contact between tool and workpiece surface up to last moments of a cutting process.

We can see that plastic deformation of a nickel alloy is higher than of the titanium alloy Ti-GR2. This is mainly due to the composition of the material because nickel alloy contains a high proportion of copper.

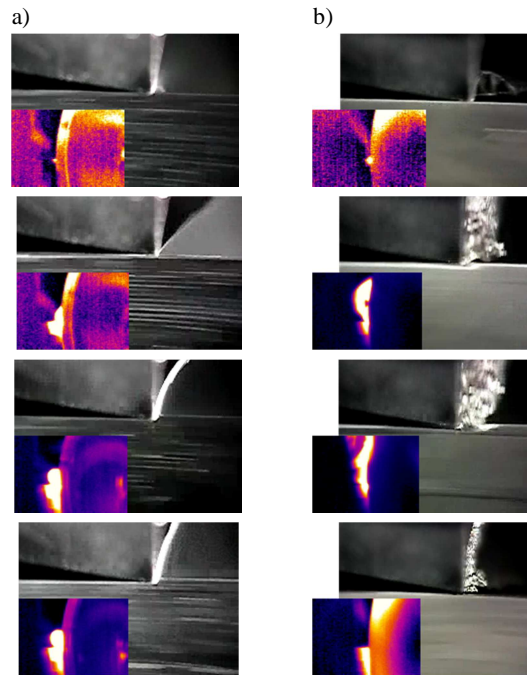


Fig. 11. Course of turning – real and thermal view:
a) Ti-GR2, b) Monel alloy 400

4.2. Courses of components of cutting force

Courses of components of cutting forces show that the titanium alloy has lower deformations in turning than nickel alloy. That was evident from visual monitoring (Fig. 12), it was confirmed in courses of cutting forces.

Sinusoidal curves in courses point to waves of stress, which is the periodic deformation in the cutting zone.

F_p component of cutting force is zero for free-cutting, recorded values are due to vibrations of the machine.

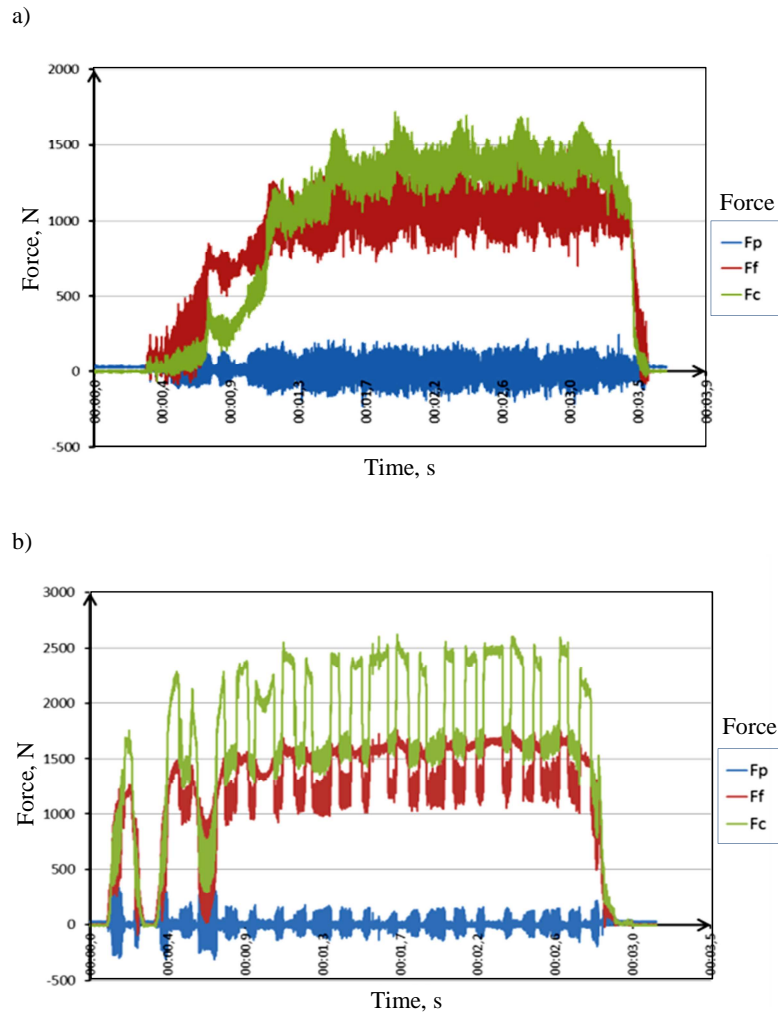
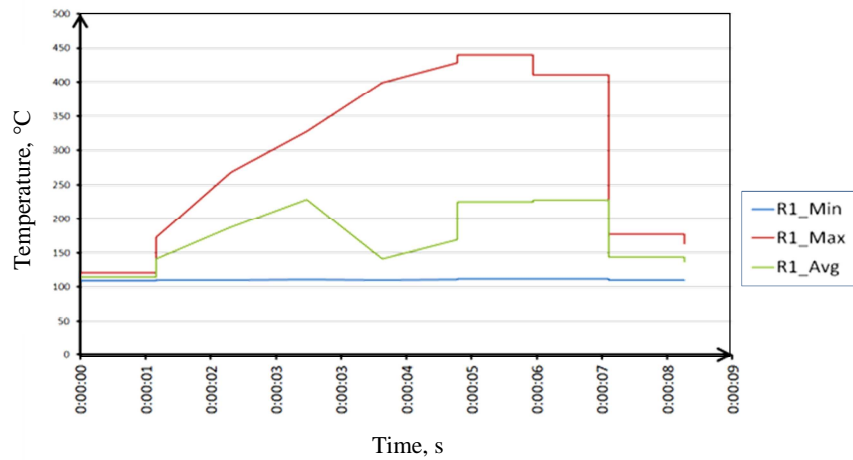


Fig. 12. Courses of components of cutting force in turning: a) titanium alloy Ti-GR2 and b) Monel alloy 400

4.3. Evolution of temperature field in the cutting zone

Temperature in the cutting zone was rising nearly parallelly with the growing cutting force. We can see that the waveforms are not completely matched. It is given by the temperature characteristics of the tested materials (Fig. 13).

a)



b)

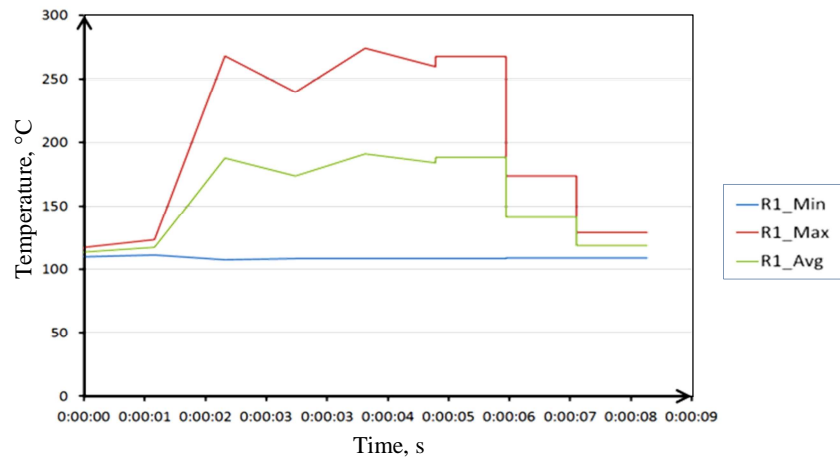


Fig. 13. Course of temperature field in cutting zone in turning of: a) titanium alloy Ti-GR2 and b) nickel alloy Monel alloy 400

5. Conclusions

This measuring system allows simultaneous measurement of the temperature and the cutting force and monitoring of deformations and chip formation in the cutting zone.

Simultaneous visual observation of these processes in cutting zone and especially visual observation of deformations in relation to thermal influence

and force effect can be a good base for better understanding of these processes and refine of simulation methods of machining processes.

The work was sponsored by funds of grant project KEGA 069ŽU-4/2011 E-learning in the field of chip-technologies and the modernisation of the workplace for the teaching of the subject for the purpose of increasing the skills of students.

References

- [1] J. BUDA, J. BÉKÉS: Teoretické základy obrábania kovov. ALFA, Bratislava 1967, 698.
- [2] M. BEŇO: Teória rezania kovov. Viena, Košice 1999.
- [3] A. CZÁN, M. NESLUŠAN: Trieskové obrábanie ťažkoobrábateľných materiálov. Rajecké Teplice 2005.
- [4] M. NESLUŠAN, S. TUREK, J. BRYCHTA, R. ČEP, M. TABAČEK: Experimentálne metódy v trieskovom obrábaní. EDIS, Žilina 2007.
- [5] L. ČEPOVA, R. ČEP, J. VALÍČEK, D. STANČEKOVÁ, L. ĎURECH, S. HLOCH, L. GREGOVA, M. HATALA: Evaluation of roundness deviation on conventional measuring device and cmm. *Technologické inžinierstvo*, (2009)2.
- [6] J. PILC, J. SALAJ, D. STANČEKOVÁ, M. ČILLIKOVÁ: Paralelné kinematické štruktúry v konštrukcii obrábacích strojov. *Strojárstvo*, (2006)2.
- [7] K. VASILKO: Teória a prax trieskového obrábania. COFIN, Prešov 2009, 35-82.
- [8] M. ŠIMKO, M. CHUPÁČ: Termovízia a jej využitie v praxi. EDIS, Žilina 2007.
- [9] K. BALCH: High frame rate electronic imaging, Motion Video Products, 1999.
- [10] R. JONES: Motion engineering company. highspeedimaging.com [online: 10th January 2009] http://highspeedimaging.com/high-speed_camera_university.cfm.
- [11] MobIR. MobIR M8 Thermal Camera. Wuhan. Wuhan Guide Infrare Co. 2008, 66.
- [12] E.P. WHINTENTON, J.C. HEIGEL: High-speed microvideography observation of the periodic catastrophic shear event in cutting AISI 1045 steel. Gaithersburg, MD. NIST, 2009.

Received in October 2012